Polymerization Mechanism and Cross-Link Structure of Nadic End-Capped Polymers: A Quantum Mechanical and Microkinetic Investigation

Sooraj Kunnikuruvan,[†] Priya V. Parandekar,[‡] Om Prakash,[‡] Thomas K. Tsotsis,[¶] and Nisanth N. Nair[*,†]

†*Department of Chemistry, Indian Institute of Technology Kanpur, Kanpur 208016, India*

‡*Boeing Research & Technology, India-centre, Bangalore-560016, India*

¶*Boeing Research & Technology, Huntington Beach, CA-92647, U. S. A*

E-mail: nnair@iitk.ac.in

Phone: +91 (0)512 2596311. Fax: +91-(0)512 2596806

Supporting Information

1 Accuracy

The accuracy of the MPW1K functional was benchmarked by comparing the barriers computed with M06 functional for the step **1**→**3** (i.e. the preferred initiation step). M06 functional[1] was used here for benchmarking as this functional is known to predict the bond dissociation energies for the multi-reference database MR-MGN-BE17 accurately,.[2] Potential energy barrier computed using MPW1K functional for the step **1**→**3** was found to be overestimated by 4 kcal mol^{-1}(see Table S2).

The basis set was benchmarked using 6-311++G(d,p) basis set for the step **1**→**3**. The difference between the potential energy barrier obtained using this basis set to that of 6-31+G(d,p) basis set was found to differ by only 0.4 kcal mol^{-1}(see Table S2). Such a small difference in barrier indicates that the basis set used here is a good choice.

Table S1: Total electronic energies (in a.u.) of **1** and transition state of step **1**→**3** (**1-3**) using MPW1K/6-31+G(d,p), MPW1K/6-311++G(d,p) and M06/6-31+G(d,p) level of theories.

	MPW1K/6-31+G(d,p)	MPW1K/6-311++G(d,p)	M06/6-31+G(d,p)
1	-784.449219892	-784.597522853	-784.133500826
1-3	-784.380381971	-784.529243244	-784.071049627

Table S2: Difference in total electronic energies (in kcal mol^{-1}) between **1** and transition state of step **1**→**3** (**1-3**) using MPW1K/6-31+G(d,p), MPW1K/6-311++G(d,p) and M06/6-31+G(d,p) level of theories.

MPW1K/6-31+G(d,p)	MPW1K/6-311++G(d,p)	M06/6-31+G(d,p)
43.2	42.8	39.2

Table S3: Total electronic energies (in a.u.) of molecules involved in the propagation reaction of **4** and the model compound **1b** with **1** and the corresponding transition states (**TS-1-4** and **TS-1-1b**) using MPW1K/6-31+G(d,) level of theory.

1	**4**	**1b**	**TS-1-4**	**TS-1-1b**
-553.454666565	1337.86050597	-554.038828233	-1891.30147035	-1107.47845979

Table S4: Potential energy barrier (in kcal mol^{-1}) for the propagation reaction of **4** and the model compound **1b** with **1**, **P1** and **P1-model** respectively.

P1	**P1-model**
8.6	9.4

2 Derivation of Rate Expression for the Rate of Polymerization

Polymerization reactions involve three major steps; (a) initiation (b) propagation and (c) termination. This can be represented by Equation (S1)-Equation (S5).

$$\mathbf{1} \rightarrow \mathrm{R}_1^i \tag{S1}$$

$$\mathrm{R}_1^i + \mathrm{M}^j \rightarrow \mathrm{R}_2^i \tag{S2}$$

$$\mathrm{R}_2^i + \mathrm{M}^j \rightarrow \mathrm{R}_3^i \tag{S3}$$

$$\vdots$$

$$\mathrm{R}_{n-1}^i + \mathrm{M}^j \rightarrow \mathrm{R}_n^i \tag{S4}$$

$$\mathrm{R}_n^i + \mathrm{R}_m^i \rightarrow \mathrm{R}_{n+m}^i \tag{S5}$$

In the above equations, Equation (S1) represents the initiation process, where R_1^i is the radical formed from the reactant, **1**, along route i. The propagation steps are shown by Equation (S2)-Equation (S4), where M^j can be **1**, **2a** or **2b**. The termination step is shown in Equation (S5). The kinetics of polymerization can be then derived from these equations.

The rate of polymerization or the consumption of any one of the monomers (M^j) can be written as,

$$-\frac{d\left[M^j\right]}{dt} = k_p^j \left[M^j\right] \sum_n \left[R_n\right] \quad , \tag{S6}$$

where, k_p is the propagation rate constant. Applying steady state approximation for R_1, R_2, ..., R_n and taking sum of the rate expressions for all intermediates will result in the expression

$$\nu^i - k_t \left(\sum_n \left[R_n\right]\right)^2 = 0 \quad , \tag{S7}$$

where ν^i is the rate of initiation process and k_t is the rate constant for the termination process. In the above equation, $\nu^i = k_{ini}^i\left[\mathbf{1}\right]$, where, k_{ini}^i is the rate constant for the initiation.

$$\sum_n \left[R_n\right] = \left(\frac{\nu^i}{k_t}\right)^{\frac{1}{2}} \tag{S8}$$

Substituting Equation (S8) in Equation (S6),

$$-\frac{dM^j}{dt} = k_p^j \left[M^j\right] \left(\frac{\nu^i}{k_t}\right)^{\frac{1}{2}} \tag{S9}$$

3 Derivation of Rate Expression for the Radical Initiation Processes

1. Case 1:**IP1** pathway

   For case 1, the reaction follows Equation (S10).

$$R_i \underset{k_{1b}}{\overset{k_{1f}}{\rightleftharpoons}} R_1 \tag{S10}$$

Here, R_i and R_1 is equal to **1** and **3** respectively for the step **1→3** of **IP1**.

$$\text{Rate of initiation}, \nu^i = k_{1f}\,[R_i] \tag{S11}$$

2. Case 2: **IP2, IP5, IP7-9**

   For Case 2, the reaction follows Equation (S12).

$$R_i \underset{k_{1b}}{\overset{k_{1f}}{\rightleftharpoons}} R_j \underset{k_{2b}}{\overset{k_{2f}}{\rightleftharpoons}} R_2 \tag{S12}$$

   Where, R_i and R_j is equal to **1** and **2a** + **2b** for all pathways (**IP2, IP5, IP7-9**) and R_2 is equal to **3**, **17**, **21**, **25** and **27** for **IP2, IP5, IP7-9** pathways, respectively. Here,

$$\nu^i = k_{2f}\,[R_j] \tag{S13}$$

   Applying steady state approximation for R_j followed by simplification,

$$[R_j] = \frac{k_{1f}\,[R_i]}{k_{1b} + k_{2f}} \tag{S14}$$

$$\Rightarrow \nu^i = \frac{k_{2f} k_{1f}\,[R_i]}{k_{1b} + k_{2f}} \tag{S15}$$

3. Case 3: **IP4** and **IP6**

   For Case 3, the initiation reaction follows Equation (S16).

$$R_i \underset{k_{1b}}{\overset{k_{1f}}{\rightleftharpoons}} R_j \underset{k_{2b}}{\overset{k_{2f}}{\rightleftharpoons}} R_k \underset{k_{3b}}{\overset{k_{3f}}{\rightleftharpoons}} R_3 \tag{S16}$$

   Where, R_i and R_j is equal to **1** and **2a** + **2b** for both pathways (**IP4** and **IP6**); R_2 is equal to **11**, **16** for **IP4** and **IP6** respectively; R_3 is equal to **12** and **17** for **IP4** and **IP6** respectively. Here,

$$\nu^i = k_{3f}\,[R_k] \tag{S17}$$

Applying steady state approximation for R_j and R_k followed by simplification,

$$[\mathrm{R}_k] = \frac{k_{1\mathrm{f}} k_{2\mathrm{f}} [\mathrm{R}_i]}{k_{1\mathrm{b}} k_{2\mathrm{b}} + k_{3\mathrm{f}}(k_{1\mathrm{b}} + k_{2\mathrm{f}})} \tag{S18}$$

$$\Rightarrow \nu^i = \frac{k_{1\mathrm{f}} k_{2\mathrm{f}} k_{3\mathrm{f}} [\mathrm{R}_i]}{k_{1\mathrm{b}} k_{2\mathrm{b}} + k_{3\mathrm{f}}(k_{1\mathrm{b}} + k_{2\mathrm{f}})} \tag{S19}$$

Table S5: Cross-linking pathways (**CLP**) and steps involved in each **CLP** (**Steps**) for the various propagation pathways studied.

CLP	Steps
CLP1	$\mathbf{1 \rightarrow 3 \xrightarrow{1} \xrightarrow{1}}$
CLP2	$\mathbf{1 \rightarrow 3 \xrightarrow{2a} \xrightarrow{2a}}$
CLP3	$\mathbf{1 \rightarrow 3 \xrightarrow{2b} \xrightarrow{2b}}$
CLP4	$\mathbf{1 \rightarrow 2a + 2b \rightarrow 3 \xrightarrow{1} \xrightarrow{1}}$
CLP5	$\mathbf{1 \rightarrow 2a + 2b \rightarrow 3 \xrightarrow{2a} \xrightarrow{2a}}$
CLP6	$\mathbf{1 \rightarrow 2a + 2b \rightarrow 3 \xrightarrow{2b} \xrightarrow{2b}}$
CLP7	$\mathbf{1 \rightarrow 7 \xrightarrow{1} \xrightarrow{1}}$
CLP8	$\mathbf{1 \rightarrow 7 \xrightarrow{2a} \xrightarrow{2a}}$
CLP9	$\mathbf{1 \rightarrow 7 \xrightarrow{2b} \xrightarrow{2b}}$
CLP10	$\mathbf{1 \rightarrow 2a + 2b \xrightarrow{1} 11 \xrightarrow{2b} 12 \xrightarrow{1} \xrightarrow{1}}$
CLP11	$\mathbf{1 \rightarrow 2a + 2b \xrightarrow{1} 11 \xrightarrow{2b} 12 \xrightarrow{2a} \xrightarrow{2a}}$
CLP12	$\mathbf{1 \rightarrow 2a + 2b \xrightarrow{1} 11 \xrightarrow{2b} 12 \xrightarrow{2b} \xrightarrow{2b}}$
CLP13	$\mathbf{1 \rightarrow 2a + 2b \xrightarrow{2a} 17 \xrightarrow{1} \xrightarrow{1}}$
CLP14	$\mathbf{1 \rightarrow 2a + 2b \xrightarrow{2a} 17 \xrightarrow{2a} \xrightarrow{2a}}$
CLP15	$\mathbf{1 \rightarrow 2a + 2b \xrightarrow{2a} 17 \xrightarrow{2b} \xrightarrow{2b}}$
CLP16	$\mathbf{1 \rightarrow 2a + 2b \xrightarrow{2a} 16 \rightarrow 17 \xrightarrow{1} \xrightarrow{1}}$
CLP17	$\mathbf{1 \rightarrow 2a + 2b \xrightarrow{2a} 16 \rightarrow 17 \xrightarrow{2a} \xrightarrow{2a}}$
CLP18	$\mathbf{1 \rightarrow 2a + 2b \xrightarrow{2a} 16 \rightarrow 17 \xrightarrow{2b} \xrightarrow{2b}}$
CLP19	$\mathbf{1 \rightarrow 2a + 2b \rightarrow 21 \xrightarrow{1} \xrightarrow{1}}$
CLP20	$\mathbf{1 \rightarrow 2a + 2b \rightarrow 21 \xrightarrow{2a} \xrightarrow{2a}}$
CLP21	$\mathbf{1 \rightarrow 2a + 2b \rightarrow 21 \xrightarrow{2b} \xrightarrow{2b}}$
CLP22	$\mathbf{1 \rightarrow 2a + 2b \rightarrow 25 \xrightarrow{1} \xrightarrow{1}}$
CLP23	$\mathbf{1 \rightarrow 2a + 2b \rightarrow 25 \xrightarrow{2a} \xrightarrow{2a}}$
CLP24	$\mathbf{1 \rightarrow 2a + 2b \rightarrow 25 \xrightarrow{2b} \xrightarrow{2b}}$
CLP25	$\mathbf{1 \rightarrow 2a + 2b \xrightarrow{1} 29 \xrightarrow{1} \xrightarrow{1}}$
CLP26	$\mathbf{1 \rightarrow 2a + 2b \xrightarrow{1} 29 \xrightarrow{2a} \xrightarrow{2a}}$
CLP27	$\mathbf{1 \rightarrow 2a + 2b \xrightarrow{1} 29 \xrightarrow{2b} \xrightarrow{2b}}$

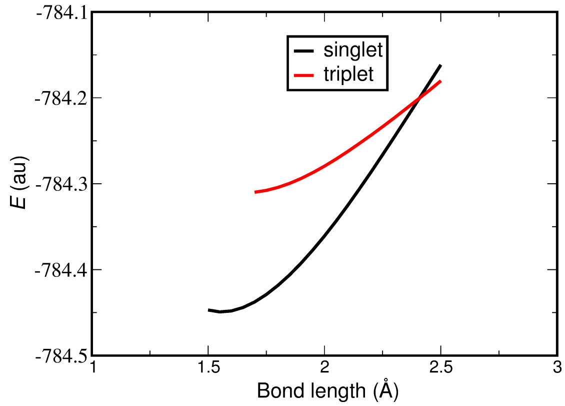

Figure S1: Singlet (black curve) and triplet (red curve) potential energy curves for the step **1**→**3** obtained using MPW1K/6-31+G(d,p) level of theory

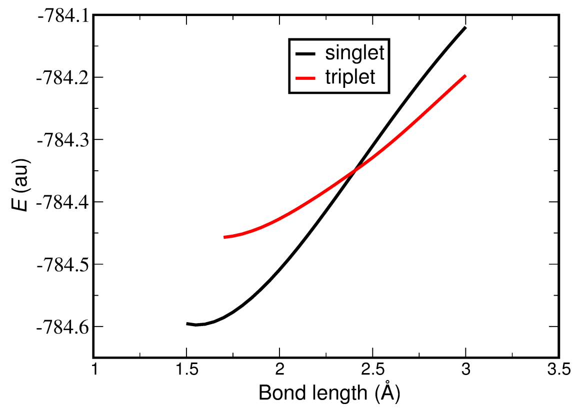

Figure S2: Singlet (black curve) and triplet (red curve) potential energy curves for the step **1**→**3** obtained using MPW1K/6-311++G(d,p) level of theory

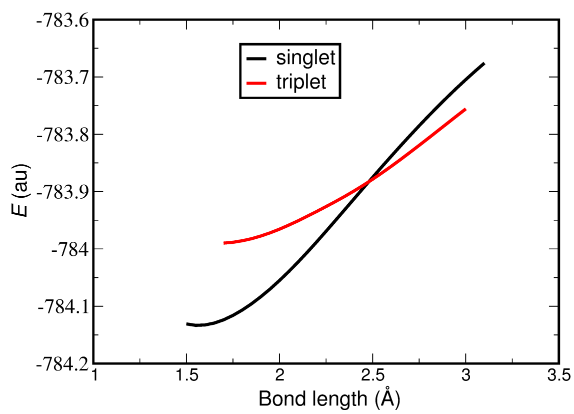

Figure S3: Singlet (black curve) and triplet (red curve) potential energy curves for the step **1**→**3** obtained using M06/6-31+G(d,p) level of theory

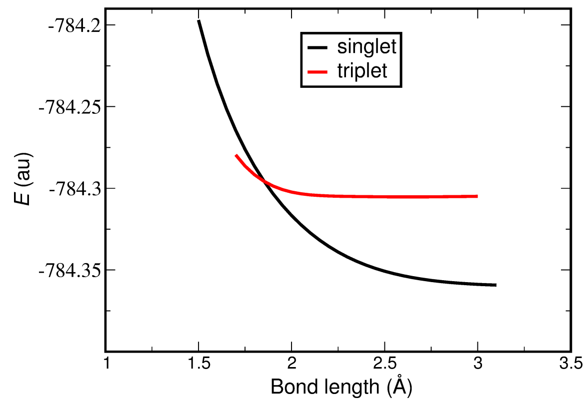

Figure S4: Singlet (black curve) and triplet (red curve) potential energy curves for the step **2a**+**2b**→**3** obtained using MPW1K/6-31+G(d,p) level of theory

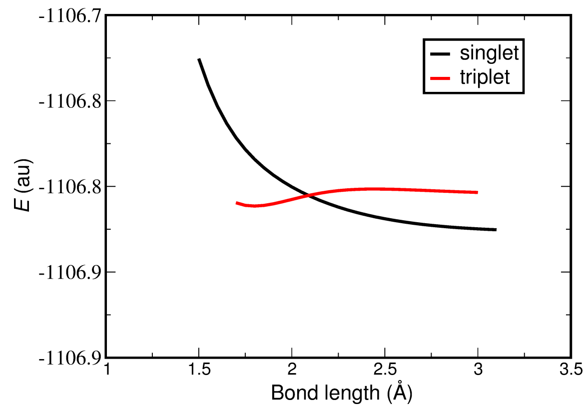

Figure S5: Singlet (black curve) and triplet (red curve) potential energy curves for the step **1**+**1**→**7** obtained using MPW1K/6-31+G(d,p) level of theory

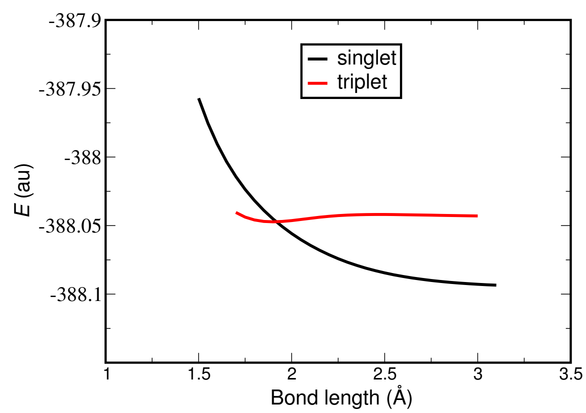

Figure S6: Singlet (black curve) and triplet (red curve) potential energy curves for the step **2a**+**2a**→**17** obtained using MPW1K/6-31+G(d,p) level of theory

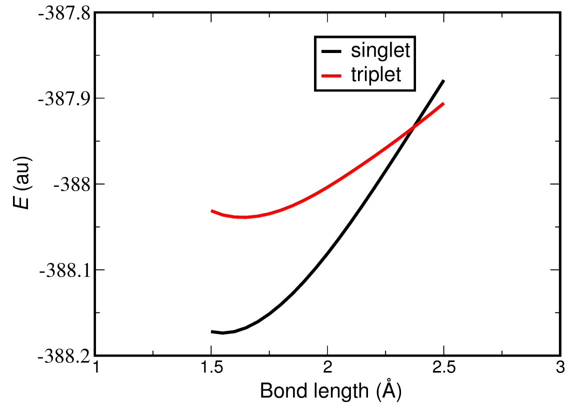

Figure S7: Singlet (black curve) and triplet (red curve) potential energy curves for the step **16**$\rightarrow$**17** obtained using MPW1K/6-31+G(d,p) level of theory

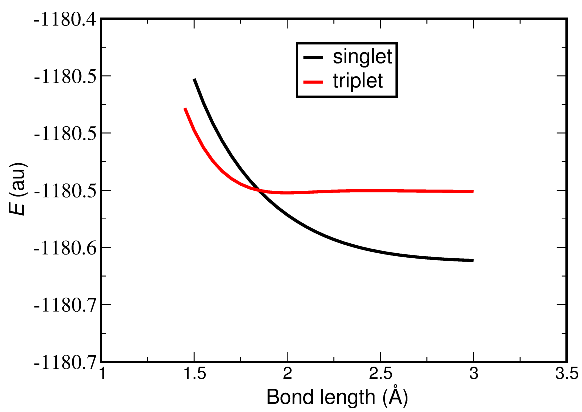

Figure S8: Singlet (black curve) and triplet (red curve) potential energy curves for the step **2b**+**2b**$\rightarrow$**21** obtained using MPW1K/6-31+G(d,p) level of theory

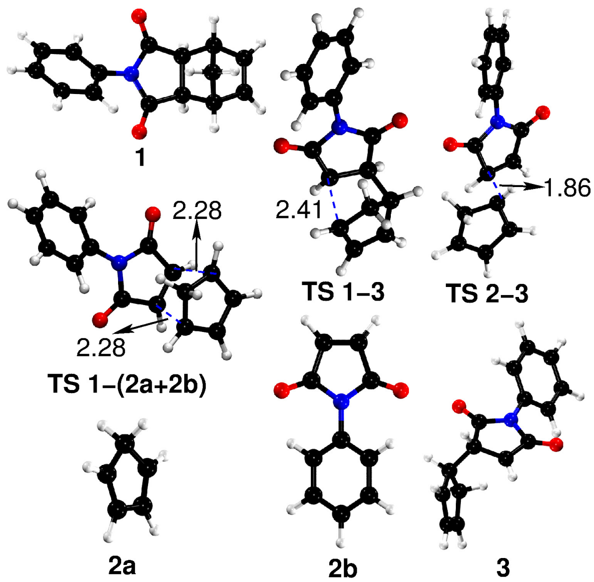

Figure S9: Optimized structures of minima and transition states along **IP1** and **IP2** pathways. Crucial distances (in Å) are shown. The transition state for any step **A**→**B** is labeled as **TS A-B**. Atom color codes: C-black, N-blue, O-red and H-white.

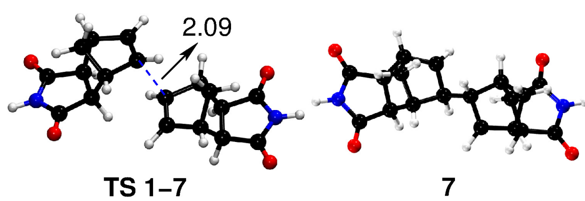

Figure S10: Optimized structures of minimum and transition state along **IP3** pathway. Color codes and other descriptions are same as that in Figure S9.

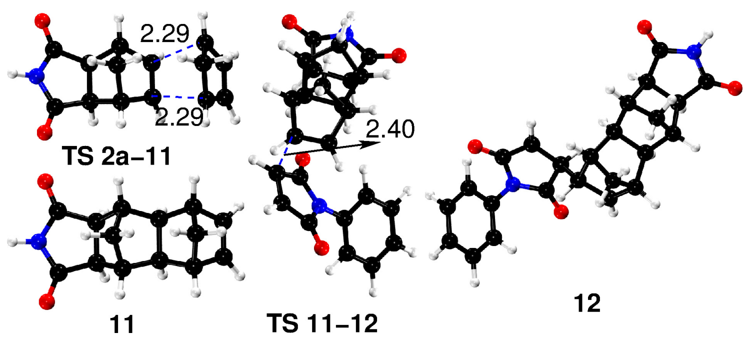

Figure S11: Optimized structures of minimum and transition state along **IP4** pathway.

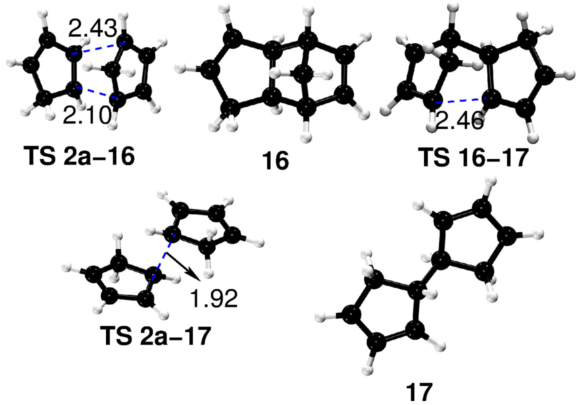

Figure S12: Optimized structures of minima and transition states along **IP5** and **IP6** pathways.

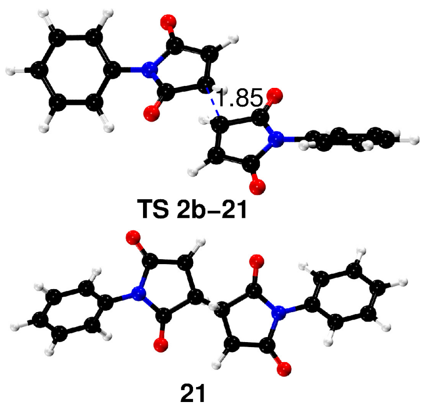

Figure S13: Optimized structures of minimum and transition state along **IP7** pathway.

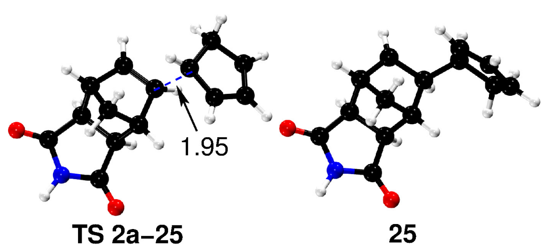

Figure S14: Optimized structures of minima and transition state along **IP8** pathway.

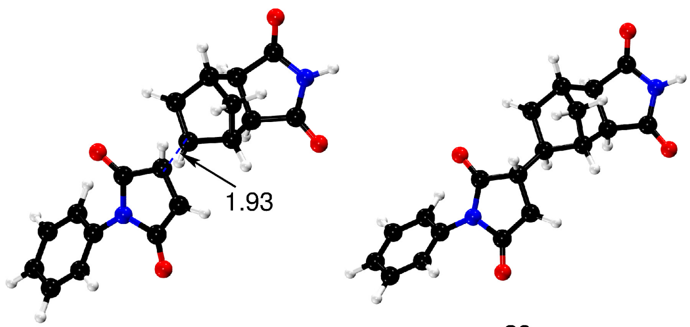

Figure S15: Optimized structures of minima and transition state along **IP9** pathway

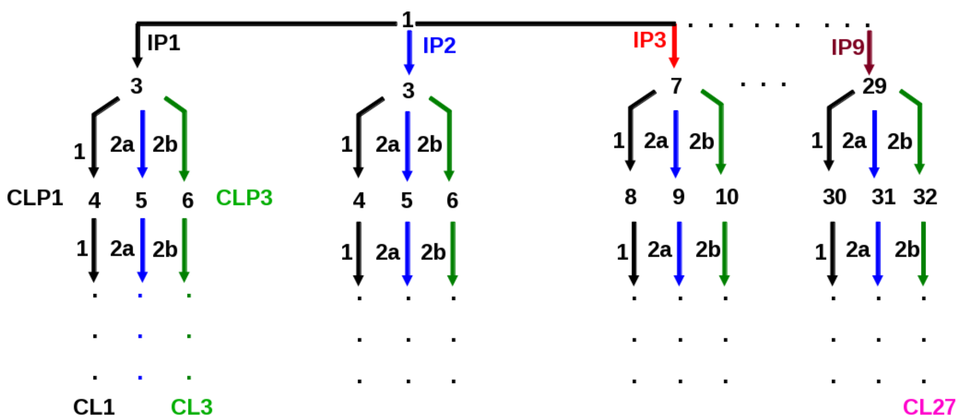

Figure S16: Scheme showing propagation pathways initiated by radicals generated along **IP1**–**IP9**. Here, **CLP**s and **CL**s have same description as given in the manuscript. The labeling scheme used here for the propagation reactions is also used in other figures and tables.

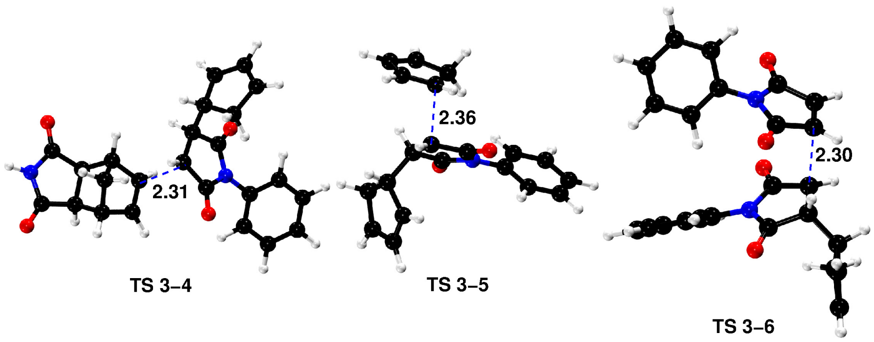

Figure S17: Optimized structures of transitions states for the propagation pathways initiated by **3**. Please see Figure S16 for the labels used for the optimized structures.

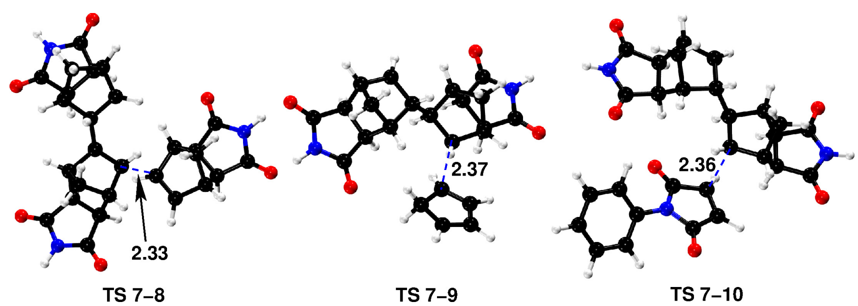

Figure S18: Optimized structures of transitions states for the propagation pathways initiated by **7**.

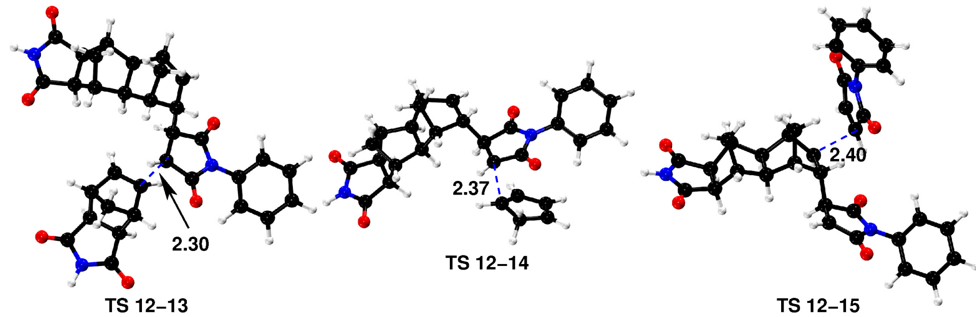

Figure S19: Optimized structures of transitions states for the propagation pathways initiated by **12**.

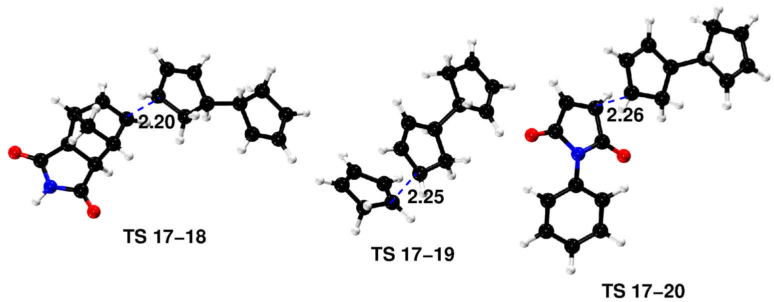

Figure S20: Optimized structures of transitions states for the propagation pathways initiated by **17**.

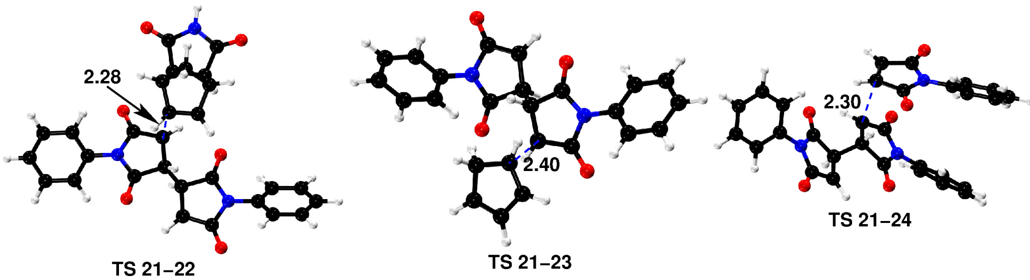

Figure S21: Optimized structures of transitions states for the propagation pathways initiated by **21**.

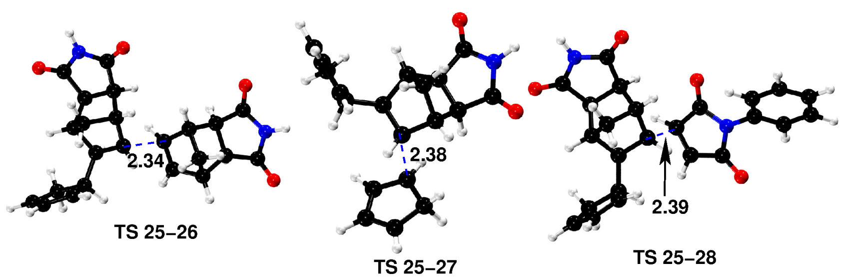

Figure S22: Optimized structures of transitions states for the propagation pathways initiated by **25**.

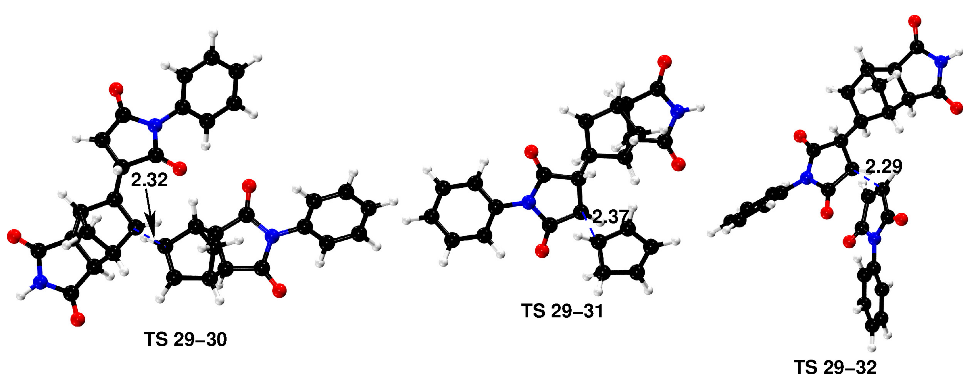

Figure S23: Optimized structures of transitions states for the propagation pathways initiated by **29**.

Table S6: Free energy (in a.u.) of all chemical structures considered in the polymerization of nadic end-cap computed at 600 K using MPW1K/6-31+G(d,p) level of theory. Note that geometry optimization was performed for both singlet and triplet state wherever applicable. For all the propagation pathways involving radicals **3**, **12**, **25** and **29**, where there are two possible reaction cites, both the possibilities were considered.

	Multiplicity, M	Free energy (a.u.)
1	1	-784.299765
1a	1	-553.365381
1-2	1	-784.228567
2a	1	-194.033110
2b	1	-590.260934
2-3	1	-784.207091
2-3	3	-784.183899
1-3	1	-784.235130
1-3	3	-784.174548
3	1	-784.235463
3	3	-784.238211
3-4a	3	-1337.539659
4a	3	-1337.578054
4b	3	-1568.513758
3-4	3	-1337.550621
4	3	-1337.596834
4c	3	-1568.531313
3-5	3	-978.225003
5	3	-978.275630
3-5a	3	-978.205912
5a	3	-978.257100
3-6a	3	-1374.444201
6a	3	-1374.480481
3-6	3	-1374.445400
6	3	-1374.496256
1-7	1	-1106.637167
7	3	-1106.660167
7-8	3	-1659.967289
8	3	-1660.014295
7-9	3	-1300.638287
9	3	-1300.696582
9a	3	-1531.630990
7-10	3	-1696.863710
10	3	-1696.914474
10a	3	-1927.848876

2a-11	1	-747.313443
11	1	-747.395175
11a	1	-978.329271
11-12	1	-1337.564399
12	3	-1337.588510
12-13a	3	-1890.886653
13a	3	-1890.943172
12-13	3	-1890.901968
13	3	-1890.947502
12-14a	3	-1531.571347
14a	3	-1531.624500
12-14	3	-1531.575315
14	3	-1531.626048
12-15	3	-1927.805482
15	3	-1927.855059
12-15a	3	-1927.798871
15a	3	-1927.846303
2a-17	1	-387.974144
17	3	-388.014075
2a-16	1	-387.986353
16	1	-388.057913
16-17	1	-387.993957
17-18	3	-941.317564
18	3	-941.358940
17-19	3	-581.988091
19	3	-582.033837
17-20	3	-978.223409
20	3	-978.259553
2b-21	1	-1180.423828
21	3	-1180.457835
21-22	3	-1733.765801
22	3	-1733.817581
21-23	3	-1374.447316
23	3	-1374.494591
21-24	3	-1770.673517
24	3	-1770.721168
2a-25	3	-747.313988
25	3	-747.334683
25-26a	3	-1300.640310
26a	3	-1300.679009
25-26	3	-1300.643772
26	3	-1300.699446

25-27	3	-941.317938
27	3	-941.377921
25-27a	3	-941.310546
27a	3	-941.356469
25-28	3	-1337.546852
28	3	-1337.599111
25-28	3	-1337.541700
28	3	-1337.578565
2b-29	1	-1143.542241
29	3	-1143.559407
29-30	3	-1927.800356
30	3	-1927.856369
29-30a	3	-1927.799448
30a	3	-1927.853321
29-31	3	-1337.549367
31	3	-1337.598835
29-31a	3	-1337.534338
31a	3	-1337.592664
29-32a	3	-1733.767104
32a	3	-1733.819187
29-32	3	-1733.767304
32	3	-1733.813342

Table S7: Free energy barriers, $\Delta G^{\ddagger}$ (in kcal mol^{-1}) and corresponding rate constants (in hours^{-1} or L mol^{-1} hours^{-1}) for all the elementary steps involved in the polymerization of nadic end-cap computed at 600 K using MPW1K/6-31+G(d,p) level of theory.

Step	$\Delta G^{\ddagger}$		Rate constant	
	Forward	Reverse	Forward	Reverse
1→2a+2b	44.7	41.1	2.4	48.1
1→3	40.6	1.9	73.1	9.1×10^{15}
2→3	54.6	19.5	6.0×10^{-4}	3.6×10^{9}
3→4	33.2	29.0	36271.0	1.2×10^{6}
3→4a	40.1	24.1	111.2	7.5×10^{7}
3→5	29.1	31.8	1.2×10^{6}	117362.0
3→5a	41.0	32.1	52.3	91253.3
3→6	33.7	31.9	23846.7	107920.0
3→6a	34.5	22.8	12190.4	2.2×10^{8}
1→7	58.7	14.4	2.0×10^{-5}	2.6×10^{11}
7→8	36.6	29.5	2094.4	807851.0
7→9	34.5	36.6	12190.4	2094.4

7→10	36.0	31.9	3464.4	107920.0
2→11	53.4	51.3	2.0×10^{-3}	$9.0\ \times10^{-3}$
11→12	57.5	15.1	5.1×10^{-5}	1.4×10^{11}
12→13	32.6	28.6	59995.3	1.7×10^{6}
12→13a	42.2	35.5	19.1	5269.3
12→14	29.1	31.8	1.1×10^{6}	117362.0
12→14a	31.5	33.4	150941.0	30669.5
12→15	27.6	31.1	4.0×10^{6}	211111.0
12→15a	31.7	29.8	127630.0	628134.0
2a→17	57.8	25.1	$4.0\ \times10^{-5}$	3.2×10^{7}
2a→16	50.1	44.9	$0.03.0\ \times10^{-2}$	2.0
16→17	40.1	12.6	111.2	1.2×10^{12}
17→18	38.8	26.0	330.9	1.5×10^{7}
17→19	37.1	28.7	1377.0	1.6×10^{6}
17→20	32.4	22.7	70952.8	2.4×10^{8}
2b→21	61.5	21.3	1.8×10^{-6}	7.8×10^{8}
21→22	36.0	32.5	3464.4	65244.4
21→23	27.4	29.7	4.7×10^{6}	683091.0
21→24	28.4	29.9	2.0×10^{6}	577599.0
2a→25	53.0	13.0	2.0×10^{-3}	8.3×10^{11}
25→26	35.3	34.9	6231.7	8715.9
25→26a	37.5	24.3	984.5	6.3×10^{7}
25→27	31.3	37.6	178508.0	905.3
25→27a	35.9	28.8	3767.5	1.5×10^{6}
25→28	30.6	32.8	321102.0	50730.0
25→28a	33.8	23.1	21928.1	1.7×10^{8}
2b→29	52.8	10.8	3.0×10^{-3}	5.2×10^{12}
29→30	36.9	35.1	1628.5	7369.9
29→30a	37.5	33.8	984.5	21928.1
29→31	27.1	31.0	6.0×10^{6}	229582.0
29→31a	36.5	36.6	2277.7	2094.4
29→32	33.3	28.9	33352.9	1.3×10^{6}
29→32a	33.4	32.7	30669.5	55168.4

Full Citation of Reference 37

Gaussian 09, Revision B.01, M. J. Frisch, G. W. Trucks, H. B. Schlegel, G. E. Scuseria, M. A. Robb, J. R. Cheeseman, G. Scalmani, V. Barone, B. Mennucci, G. A. Petersson, H. Nakatsuji, M. Caricato, X. Li, H. P. Hratchian, A. F. Izmaylov, J. Bloino, G. Zheng, J. L. Sonnenberg, M. Hada, M. Ehara, K. Toyota, R. Fukuda, J. Hasegawa, M. Ishida, T.

Nakajima, Y. Honda, O. Kitao, H. Nakai, T. Vreven, J. A. Montgomery, Jr., J. E. Peralta, F. Ogliaro, M. Bearpark, J. J. Heyd, E. Brothers, K. N. Kudin, V. N. Staroverov, T. Keith, R. Kobayashi, J. Normand, K. Raghavachari, A. Rendell, J. C. Burant, S. S. Iyengar, J. Tomasi, M. Cossi, N. Rega, J. M. Millam, M. Klene, J. E. Knox, J. B. Cross, V. Bakken, C. Adamo, J. Jaramillo, R. Gomperts, R. E. Stratmann, O. Yazyev, A. J. Austin, R. Cammi, C. Pomelli, J. W. Ochterski, R. L. Martin, K. Morokuma, V. G. Zakrzewski, G. A. Voth, P. Salvador, J. J. Dannenberg, S. Dapprich, A. D. Daniels, O. Farkas, J. B. Foresman, J. V. Ortiz, J. Cioslowski, and D. J. Fox, Gaussian, Inc., Wallingford CT, 2010.

References

(1) Zhao, Y.; Truhlar, D. G. The M06 Suite of Density Functionals for Main Group Thermochemistry, Thermochemical Kinetics, Noncovalent Interactions, Excited States, and Transition Elements: Two New Functionals and Systematic Testing of Four M06-Class Functionals and 12 Other Functionals. *Theor. Chem. Acc.* **2008**, *120*, 215–241.

(2) Yu, H. S.; He, X.; Li, S. L.; Truhlar, D. G. MN15: A Kohn-Sham Global-Hybrid Exchange-Correlation Density Functional with Broad Accuracy for Multi-reference and Single-reference Systems and Noncovalent Interactions. *Chem. Sci.* **2016**, *7*, 5032–5051.